JACS
JOURNAL OF THE AMERICAN CHEMICAL SOCIETY
pubs.acs.org/JACS
Article

Self-Assembly of Stimuli-Responsive [2]Rotaxanes by Amidinium Exchange

Oleg Borodin, Yevhenii Shchukin, Craig C. Robertson, Stefan Richter, and Max von Delius*

Cite This: J. Am. Chem. Soc. 2021, 143, 16448−16457
Read Online
ACCESS | Metrics & More | Article Recommendations | Supporting Information

ABSTRACT: Advances in supramolecular chemistry are often underpinned by the development of fundamental building blocks and methods enabling their interconversion. In this work, we report the use of an underexplored dynamic covalent reaction for the synthesis of stimuli-responsive [2]rotaxanes. The formamidinium moiety lies at the heart of these mechanically interlocked architectures, because it enables both dynamic covalent exchange and the binding of simple crown ethers. We demonstrated that the rotaxane self-assembly follows a unique reaction pathway and that the complex interplay between crown ether and thread can be controlled in a transient fashion by addition of base and fuel acid. Dynamic combinatorial libraries, when exposed to diverse nucleophiles, revealed a profound stabilizing effect of the mechanical bond as well as intriguing reactivity differences between seemingly similar [2]rotaxanes.

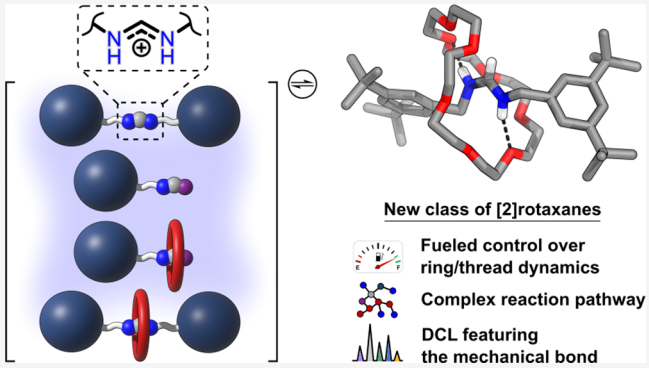

INTRODUCTION

Over the past two decades, [2]rotaxanes have found diverse uses, ranging from (stereo)selective synthesis and catalysis[1] to molecular machines,[2] the stabilization of reactive groups,[1c,2b,3] sequence-specific peptide synthesis,[4] supramolecular medicinal chemistry,[5] materials chemistry,[6] and optoelectronics.[3i,7] Future progress on these frontiers will likely depend on the development of methods for the synthesis of new types of mechanically interlocked compounds.[8] Recent examples to this end include a concave−convex $\pi-\pi$-template approach,[9] the strategic use of covalent templates based on C−Si[10] or C−O bonds,[11] organometallic macrocycles,[3h] a metal-free active template approach,[12] and hydrogen bond and halogen bond assisted anion templation.[3j,13]

Dynamic covalent chemistry (DCvC)[14] has been employed extensively for the preparation of [2]rotaxanes, [2]catenanes, and more complex mechanically interlocked architectures (MIAs).[3j,14e,15] Arguably the most popular reversible organic reaction for the preparation of MIAs has been the condensation of aldehydes with primary amines that gives rise to imines.[15f,h,k,16] This dynamic covalent reaction has however often been followed by a reduction step, giving rise to a classic pairing of rotaxane chemistry, namely the combination of a secondary ammonium ion thread with a crown ether-type ring.[17]

Herein we report the application of the dynamic covalent reaction amidinium exchange[18] (Figure 1A) for the self-assembly of [2]rotaxanes, which exhibit many features of the established ammonium/crown ether systems. In contrast to previous dynamic covalent syntheses of rotaxanes,[15d−f,j,k,16b,19] the formamidinium moiety serves both as a binding site for the

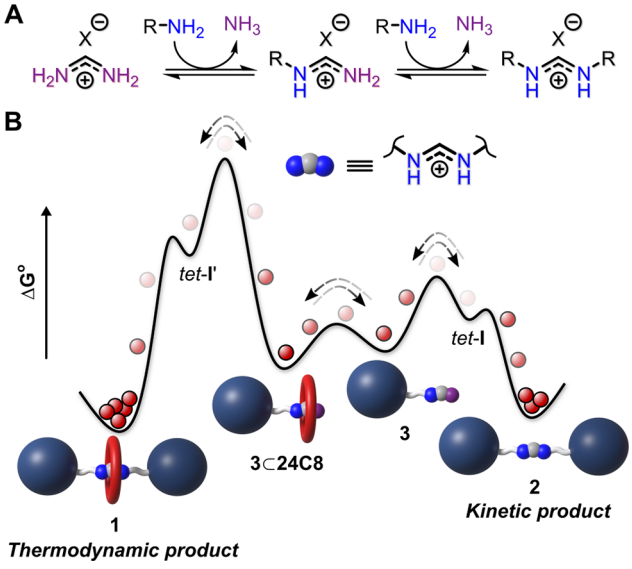

Figure 1. (A) General scheme for twofold amidinium exchange starting from formamidinium salts. (B) Qualitative free energy diagram for the self-assembly [2]rotaxanes by amidinium exchange. **24C8**: 24-crown-8. *tet*-**I**: tetrahedral intermediates. For the full reaction mechanism see Supporting Information, Scheme S16.

Received: May 20, 2021
Published: September 24, 2021

https://doi.org/10.1021/jacs.1c05230
J. Am. Chem. Soc. 2021, 143, 16448−16457

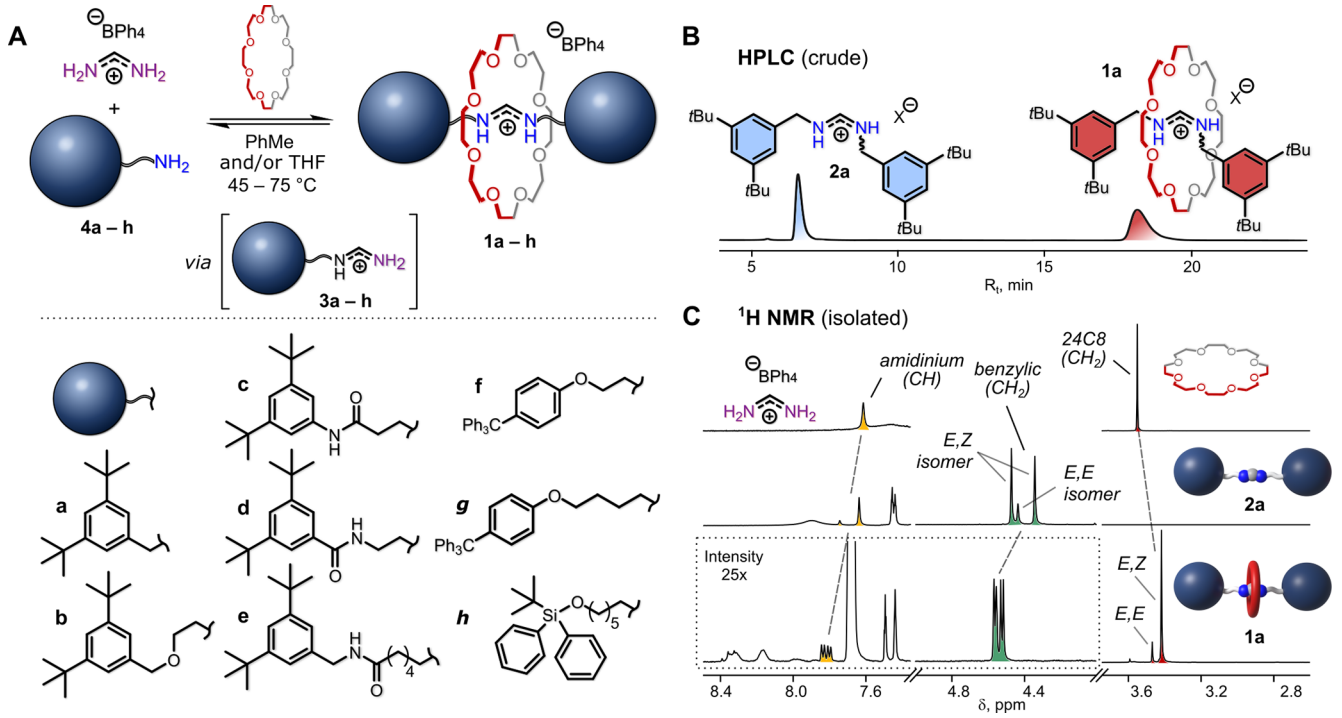

Figure 2. (A) Rotaxane self-assembly by amidinium exchange and scope of the reaction. Yields: **1a**, 36%[a] (brsm: 50%); **1b**, 21%[a]; **1c**, 16%[a] (as BArF salt); **1d**,15%[a]; **1e**, 15%[a]; **1f**, 20%[a]; **1g** 42%[b]; **1h**, 26%[b]; **1i** (2f⊂27C9), 10%[b]; **1j** (2h⊂27C9), 12%[b] (*a*, isolated yield; *b*, HPLC yield). (B) Representative HPLC chromatogram of a crude reaction mixture at equilibrium. (C) ^{1}H NMR stack plot (400 MHz, CD_3CN, 295 K) of starting materials (formamidinium tetraphenylborate and 24-crown-8), isolated thread **2a** (anion: BPh_4^-) and isolated rotaxane **1a** (anion: $BArF^-$). Both **1a** and **2a** exist in solution as a mixture of *E,E*- and *E,Z*-isomers (characteristic peaks are indicated). For chemical structure of these isomers, see Figure 3A.

ring (e.g., 24-crown-8) and as a platform for dynamic covalent exchange (Figure 1B), which makes this synthesis approach comparatively minimalistic and endows the reaction products with unusual properties. For instance, the mechanical bond between the crown ether and the *N,N′*-disubstituted formamidinium ion renders the latter much less susceptible to nucleophilic attack and dramatically slows down the interconversion between the two geometrical isomers (*E,E* and *E,Z*). We explored these features in depth by coupling the amidinium/amidine acid−base equilibrium to the fuel acid trichloroacetic acid (TCA) and by coupling dynamic combinatorial libraries (DCL) comprising six rotaxanes with the irreversible action of *N*-nucleophiles that cause the disassembly of the rotaxanes.

RESULTS AND DISCUSSION

Synthesis and Characterization of Formamidinium [2]Rotaxanes. Inspired by the seminal work of Petitjean and co-workers,[18d] we wondered if a crown ether could be coordinated during amidinium exchange, potentially affording a new type of [2]rotaxane. We also noticed recent work by Leigh and co-workers on a metal-free active template synthesis that is based on the reaction of primary amines with electrophiles inside the cavity of a crown ether.[12b,c] We therefore investigated the reaction between formamidinium tetraphenylborate (**FA·BPh$_4$**) and primary amines such as 3,5-di-*tert*-butylbenzylamine (**4a**) in the presence of 24-crown-8 (**24C8**; see Figure 2A for a general scheme). Having observed the corresponding rotaxanes **1** by tandem mass spectrometry in exploratory experiments (Supporting Information, Section 5), we proceeded with an optimization of the synthesis of **1a** and decided to vary solvent, stoichiometry, reaction temperature, base, and nucleophilic catalysts (Supporting Information, Section 3). The reaction progress was monitored by LCMS (Figure 2B). The highest molar percentage of **1a** vs **2a** (61%) was achieved when formamidinium salt, amine **4a**, and **24C8** were combined in a molar ratio of 1:2:2 in toluene at 75 °C for 3 days (Table S6). At room temperature, the reaction in THF or MeCN afforded **1a** in similar amounts (molar percentage of **1a** vs **2a** > 40%), even though the reaction took 20−40 days in this case (Tables S1−S3).

Because amidinium exchange is a reversible reaction and rotaxane **1a** and thread **2a** are not the only components of the reaction mixture (*vide infra*), rotaxane yields (isolated or HPLC) were generally lower than the above-mentioned molar percentage of 61% and fell into the range 10%−42% for the eight investigated amine stoppers (**4a−h**, Figure 2A). Isolation of the reaction products was achieved either by semipreparative HPLC or by preparative TLC, and for rotaxane **1a** we demonstrated that starting material **4a** could be recovered (yield based on recovered starting material: 50%). When the larger crown ether **27C9** was used, lower yields were observed, presumably due to weaker binding of **27C9** to the amidinium template (Supporting Information, Section 4). All isolated rotaxanes (**1a−f**) were fully characterized by ^{1}H and ^{13}C NMR spectroscopy (Supporting Information, Section 4; Figures S99−S110), and their mechanically interlocked nature was confirmed by tandem mass spectrometry (Supporting Information, Section 5). The ^{1}H NMR spectrum of **1a** (Figure 2C), as a representative example of the amidinium rotaxanes, features benzylic CH_2 signals and amidinium CH signals that are shifted downfield, compared to the corresponding signals of thread **2a**, which is indicative of interactions of those protons with the crown ether. Moreover, the amidinium CH signal in **1a** (*E,Z* isomer, *vide infra*) appears as a doublet-of-doublets, indicating that the

https://doi.org/10.1021/jacs.1c05230
J. Am. Chem. Soc. 2021, 143, 16448−16457

exchange of amidinium NH protons is slow on the NMR time scale due to hydrogen bonding with the macrocycle.

Formamidinium *E,E* and *E,Z* Isomers: Effect of the Mechanical Bond in Solution and the Solid State. In solution, both **1a** and **2a** exist as a mixture of *E,Z*- and *E,E*-isomers, as can be clearly seen from the ^{1}H NMR spectra (Figure 2C; see Supporting Information, Section 8 for NMR studies of the isomerization equilibria). In solution and for the case of weakly coordinating counterions (e.g., PF_6^- or $BArF^-$), amidinium ions adopt mainly the *E,Z*-configuration (Supporting Information, Sections 8.1 and 8.2) and this rule applies to both rotaxanes **1** and threads **2**. However, there is a striking difference between isomerization rates between the threads and their mechanically interlocked analogues: while noninterlocked amidinium ions undergo relatively fast *E,E*/*E,Z* isomerization, with a rate constant about 1.3 s^{-1} (Figures S51–S53; Table S23) at room temperature, isomerization in the amidinium rotaxanes is extremely slow: 0.006 s^{-1} at room temperature (Figures S51, S54, S56; Table S23).

The binding of shape-complementary anions is known to affect the *E,E*/*E,Z* equilibrium. For instance, it has been established that amidines strongly bind carboxylic acids ($K_a \approx 10^8$ M^{-1} in $CDCl_3$)[18d,20] and, in the case of *N,N′*-disubstituted amidines, form rigid salt bridges with well-defined *E,E* geometry.[18d] This property of amidines has been widely used in the field of supramolecular chemistry and materials science to construct sophisticated molecular architectures.[21] In agreement with this precedence, we found that *N,N′*-disubstituted amidinium ions (e.g., threads **2**) with weakly coordinating anions exhibit mainly *E,Z* geometry in solution and that addition of carboxylates led to immediate and full switching to the *E,E* geometry and formation of the salt bridge (Scheme S20, Figure S58). In stark contrast, addition of a carboxylate to a solution of rotaxane **1a** did not induce any significant shift from the *E,Z* to the *E,E* isomer, even though ^{1}H NMR spectroscopy indicated unspecific binding between carboxylate and **1a** (Scheme S21, Figure S59). This unusual behavior of mechanically interlocked amidinium ions indicates that adopting the *E,E* geometry is highly unfavorable in the presence of a surrounding crown ether.

In the solid state, literature reports suggest that *N,N′*-disubstituted formamidinium ions adopt an *E,E*-configuration (Figure 3A).[22] Therefore, we were curious whether the mechanically interlocked crown ether also alters this fundamental structural property of the formamidinium ion. To our delight, we were able to obtain single crystals of both thread **2a** (Figure 3B; BPh_4^- salt) and the corresponding rotaxane **1a** (Figure 3C, $BArF^-$ salt), and investigate their structures by X-ray diffraction. As expected, thread **2a** crystallized predominantly as the *E,E* isomer (Supporting Information, Section 11). However, rotaxane **1a** crystallized exclusively in the *E,Z*-configuration, which confirmed our previous conclusion about the high instability of the *E,E*-isomer inside the cavity of the crown ether ring. In **1a**, the amidinium moiety forms two N–H···O hydrogen bonds with the crown ether (H···O bond lengths are 2.04 and 2.20 Å). It is worth mentioning that the amidinium C–H group also forms a weak bifurcated C–H···O hydrogen bond with the crown ether (H···O bond lengths are 2.47 Å and 2.76 Å). This bifurcated hydrogen bond is, however, much longer (on average) than the corresponding bifurcated C–H···O hydrogen bonds in a complex between our formamidinium (**FA**) starting material and **24C8** (H···O bond lengths are 2.34 Å and 2.46 Å), where **FA** can perfectly fit inside the cavity of **24C8** and form in total five hydrogen bonds (including the three-centered one) with the crown ether (Figure 3D).

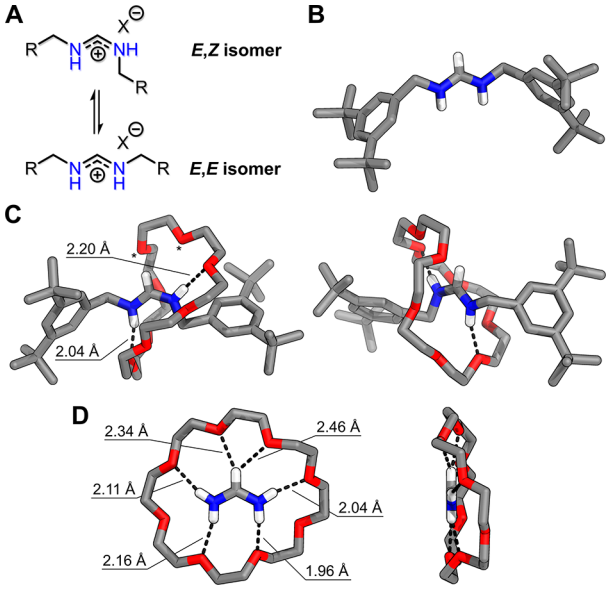

Figure 3. (A) Structure of the formamidinium *E,Z* and *E,E* isomers. (B) Crystal structure of thread **2a** (anion: BPh_4^-). (C) Crystal structure of rotaxane **1a** (anion: $BArF^-$); two different views. In the left structure, two oxygen atoms that form weak hydrogen bonds C–H···O (2.47 and 2.76 Å) with the amidinium moiety are marked with asterisks. (D) Crystal structure of a hydrogen-bonded complex between formamidinium and **24C8** (anion: BPh_4^-); two different views. Counterions and nonamidinium hydrogen atoms are omitted for clarity. Dotted lines represent hydrogen bonds.

Controlling Rotaxane Thermodynamics and Kinetics by Addition of a Chemical Fuel. We reasoned that deprotonation of the amidinium moiety in our rotaxanes would essentially shut down binding of the crown ether ring to the thread, which would be analogous to rotaxanes based on secondary ammonium ions. Indeed, upon addition of strong base NBu_4OH to rotaxane **1a**, we observed by ^{1}H NMR spectroscopy that benzylic, *tert*-butyl, and crown ether signals turned into broad singlets, indicative of relatively fast exchange between possible configurational and (co)conformational isomers on the NMR time scale (Schemes S17 and S22, Figure S60). Given the difficulty of deprotonation of ammonium-based rotaxanes,[23] the interconversion between the isomers might be further facilitated by the tautomeric equilibria induced by residual amounts of the base (HO^-).[24] As expected, addition of acetic acid (1 equiv) restored the sharp signals belonging to the original *E,Z*- and *E,E*-isomers, which due to the mechanical bond undergo slow exchange (*vide supra*).

The rotaxanes reported herein therefore exist in two states:

(i) The protonated amidinium state, where the ring is associated with the thread (K_a ca. 30 M^{-1} in CD_3CN was determined for a comparable pseudorotaxane; Supporting Information, Section 6.3) and *E,Z*/*E,E* isomerization is slow.

(ii) The deprotonated state of the thread, where binding between amidine and crown ether is negligible (K_a < 1 M^{-1} in CD_3CN was estimated by host–guest titration with a pseudorotaxane; Supporting Information, Section 6.4) and configurational (*E*/*Z*) and/or (co)-conformational dynamics are much faster compared to the protonated state.

https://doi.org/10.1021/jacs.1c05230
J. Am. Chem. Soc. 2021, 143, 16448–16457

While acid−base control of binding is a common feature of [2]rotaxanes, not least those based on secondary ammonium ions, acid−base control of thread isomerization is underexplored, because most of the studies of rotaxanes focus on either ring shuttling or pirouetting motions.[1c,25] The new rotaxane motif described herein therefore exhibits a feature that has made the crown ether/ammonium couple very popular especially for the design of molecular machines,[26] while also offering something different.

Inspired by recent reports from the groups of Takata, Di Stefano, Leigh, and Schmittel,[27] we decided to investigate whether a chemical fuel—trichloroacetic acid (TCA)—could be used to generate the strongly binding protonated state in a transient fashion. According to this reasoning, the amidine rotaxane, where the interconversion between configurational and (co)conformational isomers is fast, would be protonated by TCA, thus bringing the rotaxane into the state where interconversion between *E,Z*- and *E,E*-isomers is slowed by the ring. The trichloroacetate anion would then gradually decompose into CO_2 and $CHCl_3$, while the rotaxane is deprotonated into the original state (Figure 4A). In a proof-of-concept experiment, we added TCA to deprotonated rotaxane **1b** and observed in the ^{1}H NMR spectrum the expected splitting of broad singlets corresponding to benzylic, aromatic, and *tert*-butyl protons (Figure 4B; Scheme S23, Figures S61, S62). After 1 h at 40 °C, the original broad singlets were restored, indicating that the rotaxane was again in the deprotonated form. This cycle could be repeated at least three times, indicating that the underlying chemistry is sufficiently robust to find uses in molecular machines.

Complexity of the Reaction Pathway toward the Amidinium [2]Rotaxanes. While optimizing the reaction conditions of the rotaxane synthesis by the amidinium exchange, we were initially puzzled by the observation that rotaxane yields did not exceed 30−40% despite our best optimization efforts. Careful analysis of the reaction pathway, including host−guest titrations of key intermediate species, helped to shed light on our difficulties to obtain yields greater than 40%.

During the rotaxane self-assembly, **24C8** strongly binds to the unsubstituted formamidinium ion (K_a = 9.5 × 10^3 M^{-1} in CD_3CN at 295 K; Supporting Information, Section 6.1; crystal structure, Figure 3D) and less strongly to the key reaction intermediate−half-thread **3** ($K_a \approx 10^2$ M^{-1} in CD_3CN at 295 K; Supporting Information, Section 6.2; for general structure, see Figure 2A). This leads to the decreased reactivity of the amidinium moiety toward amines, since **24C8** sterically hinders the electrophilic reaction center on the amidinium moiety and presumably also reduces its electrophilicity due to hydrogen bonding. As a consequence, the free thread forms much faster than the rotaxane. However, the reversibility of amidinium exchange eventually leads to rotaxane formation, since *N,N′*-disubstituted amidinium ions exhibit (weak) binding to **24C8** (K_a ca. 30 M^{-1} in CD_3CN at 295 K; Supporting Information, Section 6.3), thus making the rotaxane a thermodynamic product.

Even though the reasoning from the last paragraph might explain the slow rate of rotaxane formation, it does *not* explain why the amidinium rotaxanes cannot be formed in higher yields. To understand this issue, we thought that perhaps all chemical transformations that occur during self-assembly need to be considered (Figure 5). Conjugate acids of both primary amine starting materials (**4**) and NH_3 as a byproduct of the reaction are more effective at binding **24C8** than amidinium species

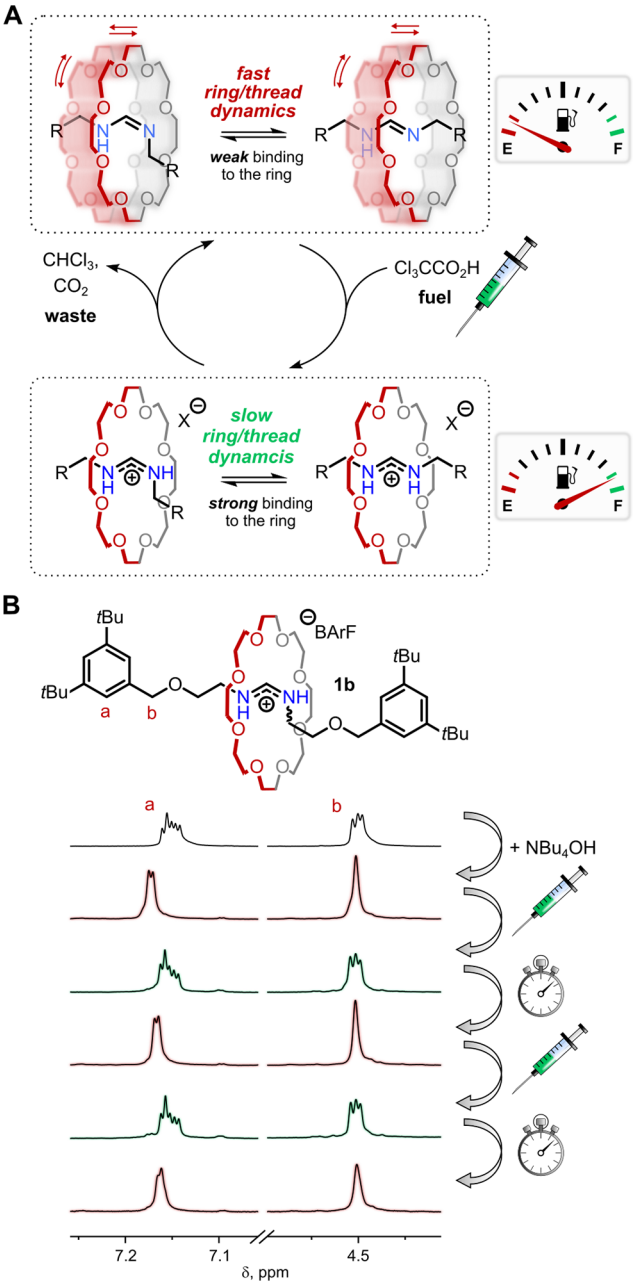

Figure 4. (A) Transient switching between two states of the amidinium rotaxane: (1) deprotonated rotaxane with fast geometry switching and (2) protonated rotaxane with slow *E*/*Z* isomerization due to hydrogen bonding to the crown ether ring. (B) Changes in ^{1}H NMR spectrum (400 MHz, CD_2Cl_2, 295 K) of rotaxane **1b** (6 mM) upon deprotonation and subsequent addition of chemical fuel −Cl_3CCO_2H (0.22 M solution in CD_2Cl_2, 1.0 equiv). Waiting time after addition of the fuel: 1 h at 40 °C. Top spectrum corresponds to the initial protonated form of **1b** (anion: $BArF^-$).

(Supporting Information, Section 6.5; Figure S33).[28] Moreover, acid−base equilibria between different nitrogen-containing species might affect not only the outcome of the host−guest equilibria but also the kinetics of amidinium exchange (considering that amidinium exchange is fast only when amidines are protonated). Overall, the reaction network comprises more than 15 different equilibria (dynamic covalent, host−guest, acid−base, and *E,Z*/*E,E*), which is unusually

https://doi.org/10.1021/jacs.1c05230
J. Am. Chem. Soc. 2021, 143, 16448−16457

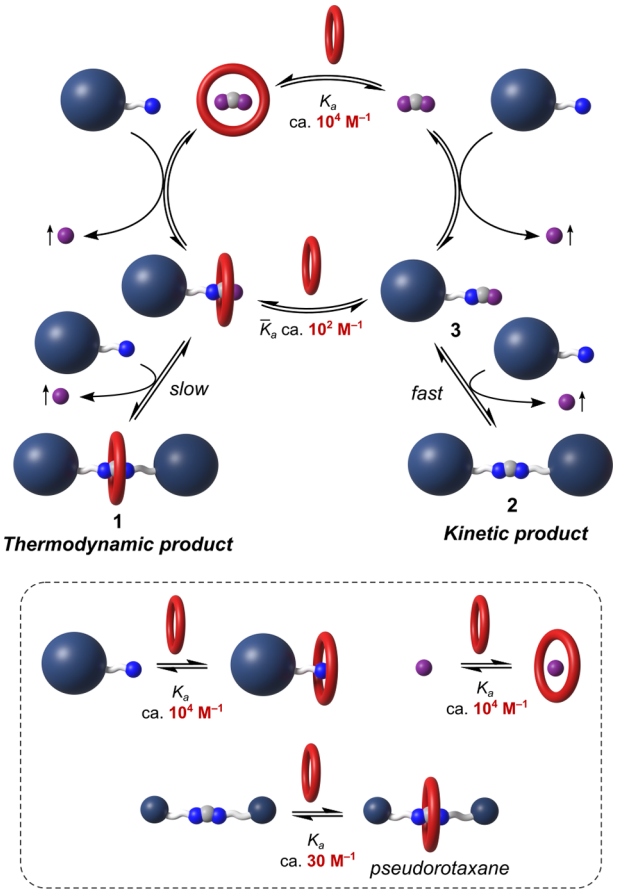

Figure 5. Proposed reaction pathway toward the amidinium rotaxanes, and overview on relevant host–guest equilibria. Acid–base equilibria are omitted for clarity. Complexation between **24C8** and nitrogen containing species (NH_3, primary amines, amidines) must mainly occur while nitrogen atoms are protonated. Association constants (K_a) for complexes NH_4^+⊂**24C8**, **FA**⊂**24C8**, and **3a**⊂**24C8** were determined in CD_3CN by host–guest titrations (Supporting Information, section 6). Association constant for a complex between protonated primary amine and **24C8** was estimated as an average between K_a for NH_4^+⊂**24C8** and for the reported complex between a secondary ammonium ion and **24C8**.[30]

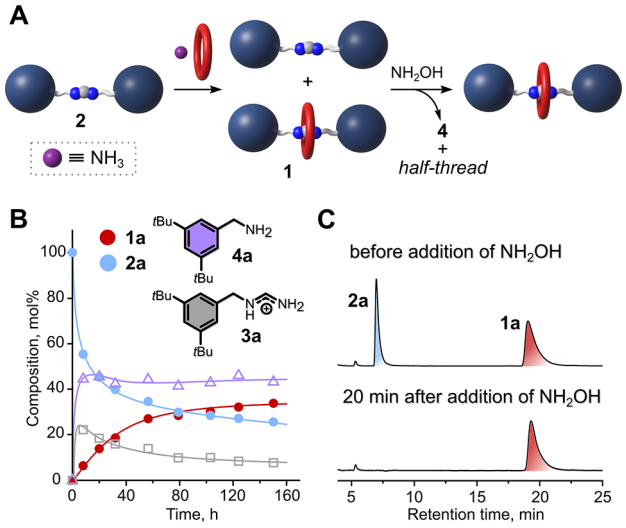

Figure 6. (A) Schematic representation of the conversion of the thread into the rotaxane and further selective degradation of the remaining thread. (B) HPLC monitoring of the conversion of thread **2a** into rotaxane **1a**. Reaction conditions: 1.0 equiv of **2a** (0.2 M), 2.6 equiv of **24C8**, 2.0 equiv of NH_3; solvent = PhMe/THF (4:6 v/v); ~65 °C. The lines are used to guide the eye. (C) HPLC chromatograms of the synthesis of **1a** before and after addition of NH_2OH (50% in H_2O, 1.25 eq. with respect to **FA·BPh$_4$**, room temperature).

complex for a rotaxane synthesis and puts the moderate observed yields into a different perspective.

To better understand the reaction pathway toward amidinium rotaxanes, we performed a series of experiments starting with an investigation of amidinium substrates other than **FA·BPh$_4$** (formamidinium acetate (**FA·OAc**), *N*,*N*′-diphenylformamidinium tetrafluoroborate, and tetrakis[3,5-bis(trifluoromethyl)phenyl]borate (**DPFA·BF$_4$** and **DPFA·BArF**), *N*,*N*′-dimethylformamidinium tetraphenylborate (**DMFA·BPh$_4$**), and *N*,*N*′-dibenzylformamidinium tetraphenylborate (**S1**)). Under standard conditions, rotaxane **1a** formed either in trace amounts (in the case of **FA·OAc** and **DPFA·BF$_4$**) or in very low yield (in the case of **DMFA·BPh$_4$**, **DPFA·BArF**, and **S1**) (Supporting Information, Sections 7.3.1–7.3.4). The amidinium exchange reaction affording noninterlocked products still proceeded smoothly from all four starting materials. In the case of **DMFA·BPh$_4$** and **FA·OAc**, we also tested the possibility to approach the same equilibria starting either from rotaxane **1a** and $MeNH_2$ or from the evolving reaction mixture and an acetate salt, respectively (Table S18 and Figure S49). In both cases, we obtained near-identical equilibrium mixtures, indicating that these systems are under thermodynamic control.

We also found that release of NH_3 has positive, yet not an essential effect on the yield of rotaxane formation (Table S14): reactions where NH_3 was released by regularly opening the reaction vessel afforded higher rotaxane yields (by ~50%) than reactions where the vessel was kept tightly closed during the course of the reaction.

The evidence described above suggests the following conclusions: (i) the rotaxane synthesis by amidinium exchange is mostly governed by thermodynamics; (ii) a successful rotaxane synthesis requires a weakly coordinating counterion, otherwise one of the thermodynamic driving forces (i.e., binding of **24C8** to the thread) becomes too small; (iii) loss of NH_3 represents an irreversible driving force for the forward rotaxane synthesis, but at the same time complete loss of NH_3 is an obstacle for conversion of the thread to the rotaxane at the end of the reaction. There is a close analogy here to the disulfide chemistry pioneered by Sanders and Otto.[29] These DCLs start from dithiols and are dynamic for a very long time until all thiols are oxidized by air to disulfides, when dynamic exchange comes to a halt.

To investigate whether the third conclusion could be leveraged to increase rotaxane yields, we decided to add ammonia to the crude self-assembly products, to test if the thread would further convert into the rotaxane. Addition of NH_3 (0.5 M solution in THF) to the crude reaction mixture, however, led only to insignificant changes of the rotaxane amount (Figures S40, S42) suggesting that the global equilibrium in the reaction system was shifted not only toward **1a** but also toward other species (half-thread **3a** and amine **4a**). The rotaxane yield could however be significantly improved (up to 47%), when we used an ammonia surrogate—$(Me_3Si)_2NH$, which is known to slowly hydrolyze to NH_3 *in situ* (Figure S43). The prospect to improve rotaxane yields by addition of $(Me_3Si)_2NH$ will be investigated systematically in future studies.

https://doi.org/10.1021/jacs.1c05230
J. Am. Chem. Soc. 2021, 143, 16448–16457

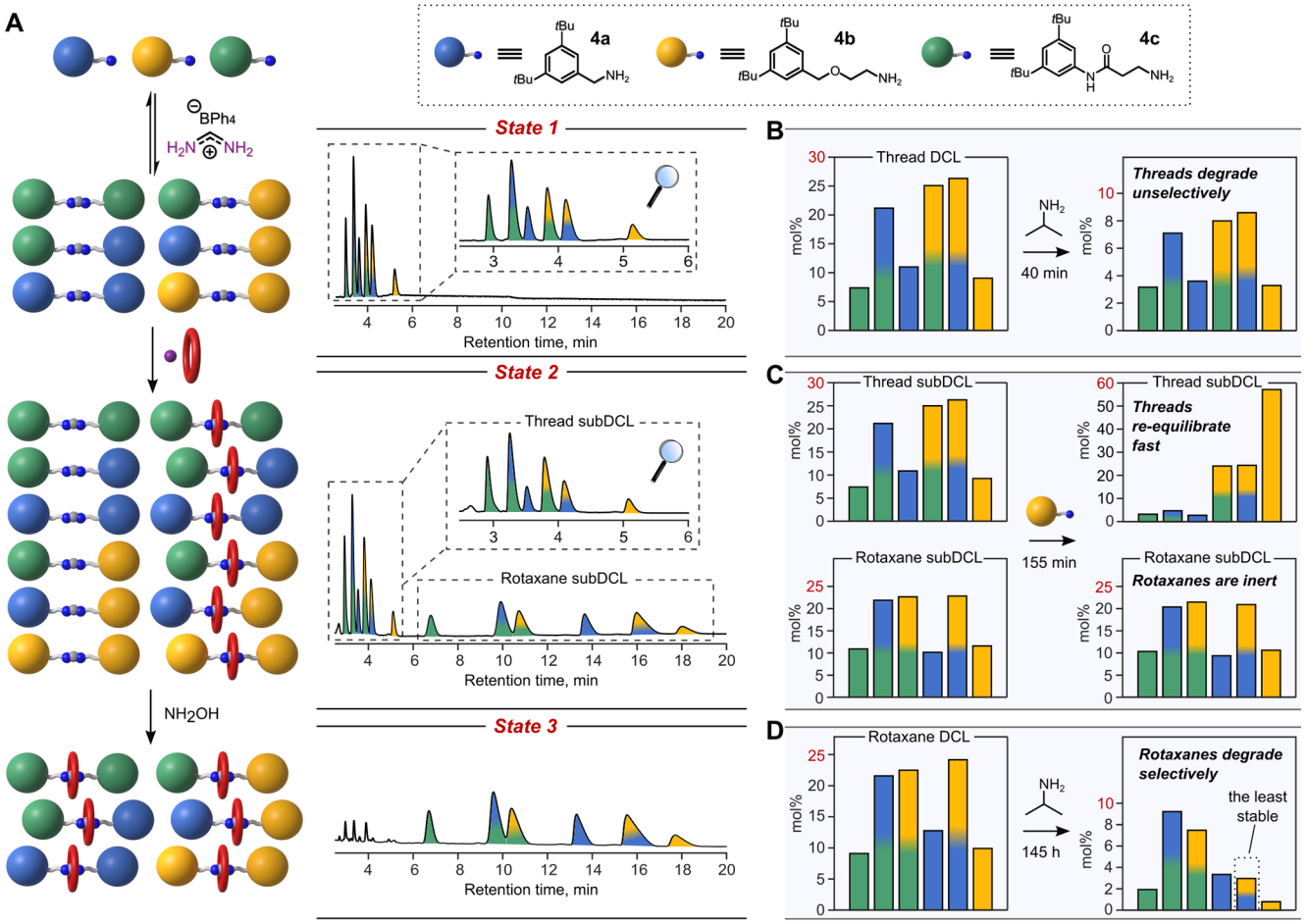

Figure 7. Synthesis and selective degradation of a dynamic combinatorial library (DCL) of amidinium rotaxanes. (A) Cartoon representation of the performed chemical transformations and corresponding HPLC chromatograms of the crude reaction mixtures. Reaction conditions: 1st step = 37 μmol of **FA·BPh$_4$**, 25 μmol of each amine, 500 μL of THF, 60 °C, 2 h; 2nd step = 74 μmol of **24C8**, 56 μmol of NH_3 (0.5 M in THF), 70 μL of PhMe, 70 °C, 100 h; 3rd step = 37 μmol NH_2OH (50% in H_2O), rt, 10 min. (B–D) Bar graphs showing changes in the distribution of the DCL members after subjecting each DCL state to an external chemical stimulus, i.e., *N*-nucleophiles (for details, see Supporting Information, Section 9.2). For these experiments, amidinium DCLs were first isolated by semipreparative HPLC and used as formate salts. In panel C, a roughly equimolar mixture of two subDCLs was used; molar percentages of the library members were calculated separately for each subDCL.

We wondered if the rotaxane formation was possible starting from thread, crown ether, and NH_3. If so, this would provide solid evidence for the reversibility of all steps in the reaction pathway. We carried out the reaction between thread **2a**, **24C8** (2.6 equiv) and NH_3 (2.0 equiv) and monitored the reaction progress by HPLC (Figure 6A and 6B, Figure S41). We found that rotaxane **1a** did gradually form and the equilibrium was reached after 6 days. Interestingly, the amount of amine **4a** reached a steady state after a few hours, while the amounts of thread **2a** and half-thread **3a** gradually decreased. Overall, the evolution of the reaction was very similar to that of a rotaxane synthesis starting from **FA·BPh$_4$**, amine **4a**, and **24C8** (Figure S40). Unexpectedly, the conversion of the thread to the rotaxane was also possible in the presence of **24C8** and amine **4a**, hence without addition of NH_3 (Table S20, entries 1 and 3; Scheme S13). This result indicates that the proposed reaction pathway (Figure 1B and Figure 5) is not the only possible one (Scheme S16), and covalent capture of the ring may occur as a result of precoordination of the ring to the amine[12b] or the thread.

Taking all the aforementioned evidence together, we conclude that the self-assembly of formamidinium rotaxanes can not be attributed to a passive template or to a metal-free active template approach,[12b,c] even though it possesses features of both. Most notably, during our amidinium rotaxane self-assembly, the crown ether ring *inhibits* the thread forming reaction, while the rotaxane can form only due to dynamic covalent exchange (Figure S50). The phenomenon that a rotaxane synthesis succeeds despite the ring component inhibiting covalent capture is rather rare and has been reported by the groups of Vögtle and Schalley.[31]

Dynamic Combinatorial Libraries of Amidinium [2]-Rotaxanes. In the rotaxanes reported herein, the amidinium moiety serves both as a binding site for the ring and as a platform for dynamic covalent exchange. This unusual architecture allows the macrocycle to affect not only supramolecular properties (e.g., amidinium anion binding) but also the kinetics of amidinium exchange (Supporting Information, Section 9.1).

A remarkable example of such a kinetic effect was observed when a crude reaction mixture after rotaxane synthesis was allowed to react with *N*-nucleophiles. Addition of strong nucleophile hydroxylamine (NH_2OH), to such a mixture of thread **2a** and rotaxane **1a**, led to complete degradation of the thread, while leaving the rotaxane intact (Figure 6A and 6C). Significant degradation of the rotaxane was only observed after prolonged reaction times (Figure S40), confirming that the crown ether ring hinders the reactive electrophilic carbon of the

https://doi.org/10.1021/jacs.1c05230
J. Am. Chem. Soc. 2021, 143, 16448–16457

amidinium moiety and further supporting the mechanistic regime described above. It is worth mentioning that selective degradation of the amidinium thread in the presence of the corresponding rotaxane also facilitated chromatographic purification of the latter, since both amidinium species are highly polar and have similar retention on a stationary phase (especially on normal phase, i.e. silica gel).

To the best of our knowledge, DCLs of MIMs, where the dynamic covalent moiety responsible for forming the thread, while also acting as binding site for the ring, have not been reported to date. We therefore proceeded with an exploration of dynamic combinatorial libraries (DCL) featuring formamidinium-based MIMs (Supporting Information, Section 9.2). In a proof-of-concept study, we used three different primary amines—**4a**, **4b**, **4c**—to prepare a DCL comprising six amidinium threads (Figure 7A, State 1). This DCL was converted into a larger DCL consisting of two sublibraries—one subDCL of threads and one subDCL of rotaxanes (Figure 7A, State 2; Figures S67, S68)—and it turned out that the two subDCLs have completely different kinetic properties. The "thread subDCL" can further "evolve" by interacting with newly introduced chemical species, while the "rotaxane subDCL" is essentially a silent observer. For instance, addition of amine **4b** led to upregulation of thread **2b** and downregulation of the other threads (Figure 7C, Figure S71). At the same time, the composition of the rotaxane subDCL remained unchanged. In another experiment, addition of NH_2OH led to fast degradation of the thread subDCL, while all the members of the rotaxane subDCL remained intact (Figure 7A, State 3).[32]

The obtained rotaxane DCL was subsequently subjected to reactions with bulky nucleophiles (e.g., isopropylamine or *tert*-butylamine) over prolonged time. Even though each rotaxane degraded by at least 50%, to our surprise, some DCL members demonstrated much higher kinetic stability (e.g., blue-green rotaxane) than others (e.g., blue-yellow rotaxane) (Figure 7D, Figures S69, S70). When considering the differences in reactivity between rotaxanes, interestingly, we did not find a correlation with the space that is available for the crown ether along the axle. Interestingly, a similar DCL of the threads (State 1) did not reveal any selectivity toward reaction with an external, bulky nucleophile (Figure 7B, Figure S69), confirming that that the mechanical bond impacts not only the thermodynamic stability of the DCL members but also their (kinetic) reactivity.

CONCLUSIONS

In conclusion, we describe a new approach for the dynamic self-assembly of [2]rotaxanes, which is based on an underexplored dynamic covalent reaction: amidinium exchange. The reaction appears to be relatively general and affords a wide range of symmetrical [2]rotaxanes in acceptable yields (up to 50% brsm yield) that may be further improved based on preliminary work using NH_3 surrogate $(Me_3Si)_2NH$. Paradoxically, the dynamic covalent nature of the reaction facilitates and prevents the rotaxane formation at the same time. On the one hand, the crown ether ring kinetically impedes the nucleophilic attack of the amidinium electrophilic carbon by a primary amine, thus turning the product forming step into the slowest step of the entire reaction network. On the other hand, it is the reversibility of amidinium exchange, which allows the whole reaction system to converge toward MIMs as the dominant products, even when the reaction is started from the isolated thread.

Amidinium rotaxanes represent an extreme case of the mechanical bond affecting fundamental kinetics and thermodynamics of a functional group.[1c,2b,3a−g,33] The rotaxanes described herein not only are surprisingly stable toward hydrolysis and the reaction with other nucleophiles but they also exhibit unusual *E,E/E,Z* isomer ratios and the interconversion between these isomers is significantly slowed down due to the presence of the interlocked crown ether. Binding of the ring can be controlled by addition of acid/base, and by using a fuel acid this process was successfully carried out in a transient manner. Overall, formamidinium/**24C8** rotaxanes represent a dynamic covalent equivalent to the well-established secondary-amine/**24C8** rotaxanes, which is why we expect uses in molecular machinery, "smart" materials, and systems chemistry.

ASSOCIATED CONTENT

Supporting Information

The Supporting Information is available free of charge at https://pubs.acs.org/doi/10.1021/jacs.1c05230.

General experimental procedures, synthesis and characterization data, MS/MS data, host−guest titrations, mechanistic studies, *E,E/E,Z* isomerization studies, crystallographic data (PDF)

Accession Codes

CCDC 2076127−2076129 contain the supplementary crystallographic data for this paper. These data can be obtained free of charge via www.ccdc.cam.ac.uk/data_request/cif, or by emailing data_request@ccdc.cam.ac.uk, or by contacting The Cambridge Crystallographic Data Centre, 12 Union Road, Cambridge CB2 1EZ, UK; fax: +44 1223 336033.

AUTHOR INFORMATION

Corresponding Author

Max von Delius − *Institute of Organic Chemistry, Ulm University, 89081 Ulm, Germany;* orcid.org/0000-0003-1852-2969; Email: max.vondelius@uni-ulm.de

Authors

Oleg Borodin − *Institute of Organic Chemistry, Ulm University, 89081 Ulm, Germany*

Yevhenii Shchukin − *Institute of Organic Chemistry, Ulm University, 89081 Ulm, Germany;* orcid.org/0000-0001-8069-189X

Craig C. Robertson − *Department of Chemistry, University of Sheffield, Brook Hill, Sheffield S3 7HF, U.K.*

Stefan Richter − *Institute of Organic Chemistry, Ulm University, 89081 Ulm, Germany*

Complete contact information is available at: https://pubs.acs.org/10.1021/jacs.1c05230

Funding

This work was supported by the Deutscher Akademischer Austauschdienst (DAAD, PhD scholarship to O.B.), the Deutsche Forschungsgemeinschaft (DFG, Emmy-Noether Grant DE1830/2-1), and the European Research Council (ERC Starting Grant 802428 - SUPRANET).

Notes

The authors declare no competing financial interest.

ACKNOWLEDGMENTS

We thank Lionel Kroner for performing XRD measurements, Dr. Udo Werz and Christian Tontsch for help with DOSY & EXSY NMR experiments, and Dr. Markus Wunderlin for performing tandem mass spectrometry experiments.

■ ABBREVIATIONS

BArF, tetrakis[3,5-bis(trifluoromethyl)phenyl]borate; DCL, dynamic combinatorial library; DCvC, dynamic covalent chemistry; EXSY, exchange spectroscopy; HPLC, high-performance liquid chromatography; MeCN, acetonitrile; MIA, mechanically interlocked architecture; MIM, mechanically interlocked molecule; NMR, nuclear magnetic resonance; PhMe, toluene; TCA, trichloroacetic acid; THF, tetrahydrofuran; TLC, thin layer chromatography; 24C8, 24-crown-8; 27C9, 27-crown-9

■ REFERENCES

(1) (a) Leigh, D. A.; Marcos, V.; Wilson, M. R. Rotaxane Catalysts. *ACS Catal.* **2014**, *4*, 4490−4497. (b) Kwamen, C.; Niemeyer, J. Functional Rotaxanes in Catalysis. *Chem. - Eur. J.* **2021**, *27*, 175−186. (c) Neal, E. A.; Goldup, S. M. Chemical consequences of mechanical bonding in catenanes and rotaxanes: isomerism, modification, catalysis and molecular machines for synthesis. *Chem. Commun.* **2014**, *50*, 5128−5142. (d) Pairault, N.; Niemeyer, J. Chiral Mechanically Interlocked Molecules − Applications of Rotaxanes, Catenanes and Molecular Knots in Stereoselective Chemosensing and Catalysis. *Synlett* **2018**, *29*, 689−698. (e) Martinez-Cuezva, A.; Saura-Sanmartin, A.; Alajarin, M.; Berna, J. Mechanically Interlocked Catalysts for Asymmetric Synthesis. *ACS Catal.* **2020**, *10*, 7719−7733. (f) Calles, M.; Puigcerver, J.; Alonso, D. A.; Alajarin, M.; Martinez-Cuezva, A.; Berna, J. Enhancing the selectivity of prolinamide organocatalysts using the mechanical bond in [2]rotaxanes. *Chem. Sci.* **2020**, *11*, 3629−3635. (g) Dommaschk, M.; Echavarren, J.; Leigh, D. A.; Marcos, V.; Singleton, T. A. Dynamic Control of Chiral Space Through Local Symmetry Breaking in a Rotaxane Organocatalyst. *Angew. Chem., Int. Ed.* **2019**, *58*, 14955−14958. (h) Heard, A. W.; Goldup, S. M. Synthesis of a Mechanically Planar Chiral Rotaxane Ligand for Enantioselective. *Catalysis. Chem.* **2020**, *6*, 994−1006. (i) Lim, J. Y. C.; Yuntawattana, N.; Beer, P. D.; Williams, C. K. Isoselective Lactide Ring Opening Polymerisation using [2]Rotaxane Catalysts. *Angew. Chem., Int. Ed.* **2019**, *58*, 6007−6011. (j) Pairault, N.; Zhu, H.; Jansen, D.; Huber, A.; Daniliuc, C. G.; Grimme, S.; Niemeyer, J. Heterobifunctional Rotaxanes for Asymmetric Catalysis. *Angew. Chem., Int. Ed.* **2020**, *59*, 5102−5107. (k) Hsueh, F.-C.; Tsai, C.-Y.; Lai, C.-C.; Liu, Y.-H.; Peng, S.-M.; Chiu, S.-H. N-Heterocyclic Carbene Copper(I) Rotaxanes Mediate Sequential Click Ligations with All Reagents Premixed. *Angew. Chem., Int. Ed.* **2020**, *59*, 11278−11282.

(2) (a) Erbas-Cakmak, S.; Leigh, D. A.; McTernan, C. T.; Nussbaumer, A. L. Artificial Molecular Machines. *Chem. Rev.* **2015**, *115*, 10081−10206. (b) Xue, M.; Yang, Y.; Chi, X.; Yan, X.; Huang, F. Development of Pseudorotaxanes and Rotaxanes: From Synthesis to Stimuli-Responsive Motions to Applications. *Chem. Rev.* **2015**, *115*, 7398−7501. (c) Aprahamian, I. The Future of Molecular Machines. *ACS Cent. Sci.* **2020**, *6*, 347−358. (d) Corra, S.; Curcio, M.; Baroncini, M.; Silvi, S.; Credi, A. Photoactivated Artificial Molecular Machines that Can Perform Tasks. *Adv. Mater.* **2020**, *32*, 1906064−1906064. (e) Qiu, Y.; Feng, Y.; Guo, Q.-H.; Astumian, R. D.; Stoddart, J. F. Pumps through the Ages. *Chem.* **2020**, *6*, 1952−1977. (f) Heard, A. W.; Goldup, S. M. Simplicity in the Design, Operation, and Applications of Mechanically Interlocked Molecular Machines. *ACS Cent. Sci.* **2020**, *6*, 117−128. (g) Amano, S.; Fielden, S. D. P.; Leigh, D. A. A catalysis-driven artificial molecular pump. *Nature* **2021**, *594*, 529−534.

(3) (a) Gassensmith, J. J.; Baumes, J. M.; Smith, B. D. Discovery and early development of squaraine rotaxanes. *Chem. Commun.* **2009**, 6329−6338. (b) Eelkema, R.; Maeda, K.; Odell, B.; Anderson, H. L. Radical Cation Stabilization in a Cucurbituril Oligoaniline Rotaxane. *J. Am. Chem. Soc.* **2007**, *129*, 12384−12385. (c) Franz, M.; Januszewski, J. A.; Wendinger, D.; Neiss, C.; Movsisyan, L. D.; Hampel, F.; Anderson, H. L.; Görling, A.; Tykwinski, R. R. Cumulene Rotaxanes: Stabilization and Study of [9]Cumulenes. *Angew. Chem., Int. Ed.* **2015**, *54*, 6645−6649. (d) Li, H.; Zhu, Z.; Fahrenbach, A. C.; Savoie, B. M.; Ke, C.; Barnes, J. C.; Lei, J.; Zhao, Y.-L.; Lilley, L. M.; Marks, T. J.; Ratner, M. A.; Stoddart, J. F. Mechanical Bond-Induced Radical Stabilization. *J. Am. Chem. Soc.* **2013**, *135*, 456−467. (e) Oku, T.; Furusho, Y.; Takata, T. Rotaxane-Stabilized Thiophosphonium Salt from Disulfide and Phosphine. *Org. Lett.* **2003**, *5*, 4923−4925. (f) Parham, A. H.; Windisch, B.; Vögtle, F. Chemical Reactions in the Axle of Rotaxanes − Steric Hindrance by the Wheel. *Eur. J. Org. Chem.* **1999**, *1999*, 1233−1238. (g) Soto, M. A.; Lelj, F.; MacLachlan, M. J. Programming permanent and transient molecular protection via mechanical stoppering. *Chem. Sci.* **2019**, *10*, 10422−10427. (h) Altmann, P. J.; Pöthig, A. A pH-Dependent, Mechanically Interlocked Switch: Organometallic [2]Rotaxane vs. Organic [3]Rotaxane. *Angew. Chem., Int. Ed.* **2017**, *56*, 15733−15736. (i) Riaño, A.; Carini, M.; Melle-Franco, M.; Mateo-Alonso, A. Mechanically Interlocked Nitrogenated Nanographenes. *J. Am. Chem. Soc.* **2020**, *142*, 20481−20488. (j) Kandrnálová, M.; Kokan, Z.; Havel, V.; Nečas, M.; Šindelář, V. Hypervalent Iodine Based Reversible Covalent Bond in Rotaxane Synthesis. *Angew. Chem., Int. Ed.* **2019**, *58*, 18182−18185. (k) Winn, J.; Pinczewska, A.; Goldup, S. M. Synthesis of a Rotaxane CuI Triazolide under Aqueous Conditions. *J. Am. Chem. Soc.* **2013**, *135*, 13318−13321.

(4) (a) De Bo, G.; Gall, M. A. Y.; Kuschel, S.; De Winter, J.; Gerbaux, P.; Leigh, D. A. An artificial molecular machine that builds an asymmetric catalyst. *Nat. Nanotechnol.* **2018**, *13*, 381−385. (b) Echavarren, J.; Gall, M. A. Y.; Haertsch, A.; Leigh, D. A.; Spence, J. T. J.; Tetlow, D. J.; Tian, C. Sequence-Selective Decapeptide Synthesis by the Parallel Operation of Two Artificial Molecular Machines. *J. Am. Chem. Soc.* **2021**, *143*, 5158−5165. (c) Lewandowski, B.; De Bo, G.; Ward, J. W.; Papmeyer, M.; Kuschel, S.; Aldegunde, M. J.; Gramlich, P. M. E.; Heckmann, D.; Goldup, S. M.; D'Souza, D. M.; Fernandes, A. E.; Leigh, D. A. Sequence-Specific Peptide Synthesis by an Artificial Small-Molecule Machine. *Science* **2013**, *339*, 189−193.

(5) (a) Biros, S.; Hof, F., Supramolecular Approaches to Medicinal Chemistry. In *Supramolecular Chemistry: From Molecules to Nanomaterials*; John Wiley & Sons, Ltd.: 2012. (b) Barat, R.; Legigan, T.; Tranoy-Opalinski, I.; Renoux, B.; Péraudeau, E.; Clarhaut, J.; Poinot, P.; Fernandes, A. E.; Aucagne, V.; Leigh, D. A.; Papot, S. A mechanically interlocked molecular system programmed for the delivery of an anticancer drug. *Chem. Sci.* **2015**, *6*, 2608−2613. (c) Fernandes, A.; Viterisi, A.; Coutrot, F.; Potok, S.; Leigh, D. A.; Aucagne, V.; Papot, S. Rotaxane-Based Propeptides: Protection and Enzymatic Release of a Bioactive Pentapeptide. *Angew. Chem., Int. Ed.* **2009**, *48*, 6443−6447. (d) Kench, T.; Summers, P. A.; Kuimova, M. K.; Lewis, J. E. M.; Vilar, R. Rotaxanes as Cages to Control DNA Binding, Cytotoxicity, and Cellular Uptake of a Small Molecule. *Angew. Chem., Int. Ed.* **2021**, *60*, 10928−10934. (e) Kimura, M.; Makio, K.; Hara, K.; Hiruma, W.; Fujita, Y.; Takata, T.; Nishio, K.; Ono, N. A Supramolecular Substance, [2] Rotaxane, Induces Apoptosis in Human Molt-3 Acute Lymphoblastic Leukemia Cells. *Drug Res. (Stuttgart, Ger.)* **2015**, *65*, 614−616. (f) Lee, J.-J.; Gonçalves, A.; Smith, B. A.; Palumbo, R.; White, A. G.; Smith, B. D. Singlet Oxygen Release and Cell Toxicity of a Chemiluminescent Squaraine Rotaxane Dye: Implications for Molecular Imaging. *Aust. J. Chem.* **2011**, *64*, 604−610. (g) Ma, X.; Zhao, Y. Biomedical Applications of Supramolecular Systems Based on Host−Guest Interactions. *Chem. Rev.* **2015**, *115*, 7794−7839. (h) Yu, G.; Wu, D.; Li, Y.; Zhang, Z.; Shao, L.; Zhou, J.; Hu, Q.; Tang, G.; Huang, F. A pillar[5]arene-based [2]rotaxane lights up mitochondria. *Chem. Sci.* **2016**, *7*, 3017−3024.

(6) (a) Mena-Hernando, S.; Pérez, E. M. Mechanically interlocked materials. Rotaxanes and catenanes beyond the small molecule. *Chem. Soc. Rev.* **2019**, *48*, 5016−5032. (b) Moulin, E.; Faour, L.; Carmona-Vargas, C. C.; Giuseppone, N. From Molecular Machines to Stimuli-Responsive Materials. *Adv. Mater.* **2020**, *32*, 1906036.

(7) (a) Pruchyathamkorn, J.; Kendrick, W. J.; Frawley, A. T.; Mattioni, A.; Caycedo-Soler, F.; Huelga, S. F.; Plenio, M. B.; Anderson, H. L. A Complex Comprising a Cyanine Dye Rotaxane and a Porphyrin Nanoring as a Model Light-Harvesting System. *Angew. Chem., Int. Ed.* **2020**, *59*, 16455−16458. (b) Qu, D.-H.; Wang, Q.-C.; Zhang, Q.-W.; Ma, X.; Tian, H. Photoresponsive Host−Guest Functional Systems. *Chem. Rev.* **2015**, *115*, 7543−7588. (c) Jia, C.; Li, H.; Jiang, J.; Wang, J.;

https://doi.org/10.1021/jacs.1c05230
J. Am. Chem. Soc. 2021, 143, 16448−16457

Chen, H.; Cao, D.; Stoddart, J. F.; Guo, X. Interface-Engineered Bistable [2]Rotaxane-Graphene Hybrids with Logic Capabilities. *Adv. Mater.* **2013**, *25*, 6752−6759. (d) Rajamalli, P.; Rizzi, F.; Li, W.; Jinks, M. A.; Gupta, A. K.; Laidlaw, B. A.; Samuel, I. D. W.; Penfold, T. J.; Goldup, S. M.; Zysman-Colman, E. Using the Mechanical Bond to Tune the Performance of a Thermally Activated Delayed Fluorescence Emitter. *Angew. Chem., Int. Ed.* **2021**, *60*, 12066−12073.

(8) Bruns, C. J.; Stoddart, J. F. *The nature of the mechanical bond: from molecules to machines*; John Wiley & Sons: 2016.

(9) Xu, Y.; Kaur, R.; Wang, B.; Minameyer, M. B.; Gsänger, S.; Meyer, B.; Drewello, T.; Guldi, D. M.; von Delius, M. Concave−Convex $\pi-\pi$ Template Approach Enables the Synthesis of [10]-Cycloparaphenylene−Fullerene [2]Rotaxanes. *J. Am. Chem. Soc.* **2018**, *140*, 13413−13420.

(10) Segawa, Y.; Kuwayama, M.; Hijikata, Y.; Fushimi, M.; Nishihara, T.; Pirillo, J.; Shirasaki, J.; Kubota, N.; Itami, K. Topological molecular nanocarbons: All-benzene catenane and trefoil knot. *Science* **2019**, *365*, 272−276.

(11) Cornelissen, M. D.; Pilon, S.; Steemers, L.; Wanner, M. J.; Frölke, S.; Zuidinga, E.; Jørgensen, S. I.; van der Vlugt, J. I.; van Maarseveen, J. H. A Covalent and Modular Synthesis of Homo- and Hetero[n]-rotaxanes. *J. Org. Chem.* **2020**, *85*, 3146−3159.

(12) (a) De Bo, G.; Dolphijn, G.; McTernan, C. T.; Leigh, D. A. [2]Rotaxane Formation by Transition State Stabilization. *J. Am. Chem. Soc.* **2017**, *139*, 8455−8457. (b) Fielden, S. D. P.; Leigh, D. A.; McTernan, C. T.; Pérez-Saavedra, B.; Vitorica-Yrezabal, I. J. Spontaneous Assembly of Rotaxanes from a Primary Amine, Crown Ether and Electrophile. *J. Am. Chem. Soc.* **2018**, *140*, 6049−6052. (c) Tian, C.; Fielden, S. D. P.; Whitehead, G. F. S.; Vitorica-Yrezabal, I. J.; Leigh, D. A., Weak functional group interactions revealed through metal-free active template rotaxane synthesis. *Nat. Commun.* **2020**, *11*, 744. (d) Orlandini, G.; Ragazzon, G.; Zanichelli, V.; Secchi, A.; Silvi, S.; Venturi, M.; Arduini, A.; Credi, A. Covalent capture of oriented calix[6]arene rotaxanes by a metal-free active template approach. *Chem. Commun.* **2017**, *53*, 6172−6174. (e) Zanichelli, V.; Ragazzon, G.; Orlandini, G.; Venturi, M.; Credi, A.; Silvi, S.; Arduini, A.; Secchi, A. Efficient active-template synthesis of calix[6]arene-based oriented pseudorotaxanes and rotaxanes. *Org. Biomol. Chem.* **2017**, *15*, 6753−6763.

(13) (a) Bunchuay, T.; Docker, A.; Martinez-Martinez, A. J.; Beer, P. D. A Potent Halogen-Bonding Donor Motif for Anion Recognition and Anion Template Mechanical Bond Synthesis. *Angew. Chem., Int. Ed.* **2019**, *58*, 13823−13827. (b) Fadler, R. E.; Al Ouahabi, A.; Qiao, B.; Carta, V.; König, N. F.; Gao, X.; Zhao, W.; Zhang, Y.; Lutz, J.-F.; Flood, A. H. Chain Entropy Beats Hydrogen Bonds to Unfold and Thread Dialcohol Phosphates inside Cyanostar Macrocycles To Form [3]Pseudorotaxanes. *J. Org. Chem.* **2021**, *86*, 4532−4546. (c) Qiao, B.; Liu, Y.; Lee, S.; Pink, M.; Flood, A. H. A high-yield synthesis and acid−base response of phosphate-templated [3]rotaxanes. *Chem. Commun.* **2016**, *52*, 13675−13678. (d) Spence, G. T.; Beer, P. D. Expanding the Scope of the Anion Templated Synthesis of Interlocked Structures. *Acc. Chem. Res.* **2013**, *46*, 571−586.

(14) (a) Rowan, S. J.; Cantrill, S. J.; Cousins, G. R. L.; Sanders, J. K. M.; Stoddart, J. F. Dynamic Covalent Chemistry. *Angew. Chem., Int. Ed.* **2002**, *41*, 898−952. (b) Corbett, P. T.; Leclaire, J.; Vial, L.; West, K. R.; Wietor, J.-L.; Sanders, J. K. M.; Otto, S. Dynamic Combinatorial Chemistry. *Chem. Rev.* **2006**, *106*, 3652−3711. (c) Jin, Y.; Yu, C.; Denman, R. J.; Zhang, W. Recent advances in dynamic covalent chemistry. *Chem. Soc. Rev.* **2013**, *42*, 6634−6654. (d) Miljanić, O. Š. Small-Molecule Systems Chemistry. *Chem.* **2017**, *2*, 502−524. (e) Cougnon, F. B. L.; Sanders, J. K. M. Evolution of Dynamic Combinatorial Chemistry. *Acc. Chem. Res.* **2012**, *45*, 2211−2221. (f) *Dynamic Covalent Chemistry: Principles, Reactions, and Applications*; John Wiley & Sons Ltd.: 2017.

(15) (a) Furlan, R. L. E.; Otto, S.; Sanders, J. K. M. Supramolecular templating in thermodynamically controlled synthesis. *Proc. Natl. Acad. Sci. U. S. A.* **2002**, *99*, 4801. (b) Haussmann, P. C.; Stoddart, J. F. Synthesizing interlocked molecules dynamically. *Chem. Rec.* **2009**, *9*, 136−154. (c) Liu, Y.; Leung, K. C.-F. Dynamic Covalent Chemistry for Synthetic Molecular Machines. *Dynamic Covalent Chemistry* **2017**, 287−319. (d) Furusho, Y.; Oku, T.; Hasegawa, T.; Tsuboi, A.; Kihara, N.; Takata, T. Dynamic Covalent Approach to [2]- and [3]Rotaxanes by Utilizing a Reversible Thiol−Disulfide Interchange Reaction. *Chem. - Eur. J.* **2003**, *9*, 2895−2903. (e) Furusho, Y.; Oku, T.; Rajkumar, G. A.; Takata, T. Dynamic Covalent Chemistry in Rotaxane Synthesis. Slipping Approach to [2]Rotaxane Utilizing Reversible Cleavage−Rebondage of Trityl Thioether Linkage. *Chem. Lett.* **2004**, *33*, 52−53. (f) Horn, M.; Ihringer, J.; Glink, P. T.; Stoddart, J. F. Kinetic versus Thermodynamic Control During the Formation of [2]Rotaxanes by a Dynamic Template-Directed Clipping Process. *Chem. - Eur. J.* **2003**, *9*, 4046−4054. (g) Au-Yeung, H. Y.; Pantoş, G. D.; Sanders, J. K. M. Dynamic Combinatorial Donor−Acceptor Catenanes in Water: Access to Unconventional and Unexpected Structures. *J. Org. Chem.* **2011**, *76*, 1257−1268. (h) Caprice, K.; Pupier, M.; Kruve, A.; Schalley, C. A.; Cougnon, F. B. L. Imine-based [2]catenanes in water. *Chem. Sci.* **2018**, *9*, 1317−1322. (i) Gianga, T.-M.; Pantoş, G. D. Structurally divergent dynamic combinatorial chemistry on racemic mixtures. *Nat. Commun.* **2020**, *11*, 3528−3528. (j) Da Silva Rodrigues, R.; Luis, E. T.; Marshall, D. L.; McMurtrie, J. C.; Mullen, K. M. Hydrazone exchange: a viable route for the solid-tethered synthesis of [2]rotaxanes. *New J. Chem.* **2021**, *45*, 4414−4421. (k) Han, X.; Liu, G.; Liu, S. H.; Yin, J. Synthesis of rotaxanes and catenanes using an imine clipping reaction. *Org. Biomol. Chem.* **2016**, *14*, 10331−10351. (l) Berrocal, J. A.; Nieuwenhuizen, M. M. L.; Mandolini, L.; Meijer, E. W.; Di Stefano, S. Copper(i)-induced amplification of a [2]catenane in a virtual dynamic library of macrocyclic alkenes. *Org. Biomol. Chem.* **2014**, *12*, 6167−6174. (m) Miljanić, O. Š.; Stoddart, J. F. Dynamic donor−acceptor [2]catenanes. *Proc. Natl. Acad. Sci. U. S. A.* **2007**, *104*, 12966.

(16) (a) Northrop, B. H.; Aricó, F.; Tangchiavang, N.; Badjić, J. D.; Stoddart, J. F. Template-Directed Synthesis of Mechanically Interlocked Molecular Bundles Using Dynamic Covalent Chemistry. *Org. Lett.* **2006**, *8*, 3899−3902. (b) Wu, J.; Leung, K. C.-F.; Stoddart, J. F. Efficient production of [*n*]rotaxanes by using template-directed clipping reactions. *Proc. Natl. Acad. Sci. U. S. A.* **2007**, *104*, 17266−17271.

(17) (a) Hsueh, S.-Y.; Cheng, K.-W.; Lai, C.-C.; Chiu, S.-H. Efficient Solvent-Free Syntheses of [2]- and [4]Rotaxanes. *Angew. Chem., Int. Ed.* **2008**, *47*, 4436−4439. (b) Vukotic, V. N.; Harris, K. J.; Zhu, K.; Schurko, R. W.; Loeb, S. J. Metal−organic frameworks with dynamic interlocked components. *Nat. Chem.* **2012**, *4*, 456−460. (c) Takata, T. Switchable Polymer Materials Controlled by Rotaxane Macromolecular Switches. *ACS Cent. Sci.* **2020**, *6*, 129−143. (d) Corra, S.; de Vet, C.; Groppi, J.; La Rosa, M.; Silvi, S.; Baroncini, M.; Credi, A. Chemical On/Off Switching of Mechanically Planar Chirality and Chiral Anion Recognition in a [2]Rotaxane Molecular Shuttle. *J. Am. Chem. Soc.* **2019**, *141*, 9129−9133.

(18) (a) Alder, R. W.; Blake, M. E.; Bufali, S.; Butts, C. P.; Orpen, A. G.; Schütz, J.; Williams, S. J. Preparation of tetraalkylformamidinium salts and related species as precursors to stable carbenes. *J. Chem. Soc., Perkin Trans. 1* **2001**, 1586−1593. (b) Díaz, D. D.; Finn, M. G. Modular synthesis of formamidines and their formation of stable organogels. *Chem. Commun.* **2004**, 2514−2516. (c) Díaz, D. D.; Lewis, W. G.; Finn, M. G. Acid-Mediated Amine Exchange of N,N-Dimethylformamidines: Preparation of Electron-Rich Formamidines. *Synlett* **2005**, *2005*, 2214−2218. (d) Capela, M. d.; Mosey, N. J.; Xing, L.; Wang, R.; Petitjean, A. Amine Exchange in Formamidines: An Experimental and Theoretical Study. *Chem. - Eur. J.* **2011**, *17*, 4598−4612.

(19) Haussmann, P. C.; Khan, S. I.; Stoddart, J. F. Equilibrating Dynamic [2]Rotaxanes. *J. Org. Chem.* **2007**, *72*, 6708−6713.

(20) (a) Ren, X.; Wang, X.; Sun, Y.; Chi, X.; Mangel, D.; Wang, H.; Sessler, J. L. Amidinium−carboxylate salt bridge mediated proton-coupled electron transfer in a donor−acceptor supramolecular system. *Org. Chem. Front.* **2019**, *6*, 584−590. (b) Kraft, A.; Peters, L.; Powell, H. R. Hydrogen-bonding between benzoic acid and an N,N′-diethyl-substituted benzamidine. *Tetrahedron* **2002**, *58*, 3499−3505.

(21) (a) White, N. G. Recent advances in self-assembled amidinium and guanidinium frameworks. *Dalton Trans.* **2019**, *48*, 7062−7068. (b) Kohlhaas, M.; Zähres, M.; Mayer, C.; Engeser, M.; Merten, C.;

https://doi.org/10.1021/jacs.1c05230
J. Am. Chem. Soc. 2021, 143, 16448−16457

Niemeyer, J. Chiral hydrogen-bonded supramolecular capsules: synthesis, characterization and complexation of C70. *Chem. Commun.* **2019**, *55*, 3298−3301. (c) Yamada, H.; Wu, Z.-Q.; Furusho, Y.; Yashima, E. Thermodynamic and Kinetic Stabilities of Complementary Double Helices Utilizing Amidinium−Carboxylate Salt Bridges. *J. Am. Chem. Soc.* **2012**, *134*, 9506−9520. (d) Yashima, E.; Ousaka, N.; Taura, D.; Shimomura, K.; Ikai, T.; Maeda, K. Supramolecular Helical Systems: Helical Assemblies of Small Molecules, Foldamers, and Polymers with Chiral Amplification and Their Functions. *Chem. Rev.* **2016**, *116*, 13752−13990.

(22) (a) Clark, G. R.; Rickard, C. E. F.; Surman, P. W. J.; Taylor, M. J. Structural and spectroscopic investigations of 1,1,3,3-tetrakis-(alkylamino)allyl cations, methylene-bis(N,N′-dialkylformamidinium) dications and related formamidine derivatives. *J. Chem. Soc., Faraday Trans.* **1997**, *93*, 2503−2507. (b) Cotton, F. A.; Haefner, S. C.; Matonic, J. H.; Xiaoping, W.; Murillo, C. A. Structural studies of formamidine compounds: from neutral to anionic and cationic species. *Polyhedron* **1997**, *16*, 541−550.

(23) Tachibana, Y.; Kawasaki, H.; Kihara, N.; Takata, T. Sequential O- and N-Acylation Protocol for High-Yield Preparation and Modification of Rotaxanes: Synthesis, Functionalization, Structure, and Intercomponent Interaction of Rotaxanes. *J. Org. Chem.* **2006**, *71*, 5093−5104.

(24) Kalz, K. F.; Hausmann, A.; Dechert, S.; Meyer, S.; John, M.; Meyer, F. Solution Chemistry of N,N′-Disubstituted Amidines: Identification of Isomers and Evidence for Linear Dimer Formation. *Chem. - Eur. J.* **2016**, *22*, 18190−18196.

(25) (a) Schröder, H. V.; Mekic, A.; Hupatz, H.; Sobottka, S.; Witte, F.; Urner, L. H.; Gaedke, M.; Pagel, K.; Sarkar, B.; Paulus, B.; Schalley, C. A. Switchable synchronisation of pirouetting motions in a redox-active [3]rotaxane. *Nanoscale* **2018**, *10*, 21425−21433. (b) Lee, Y.-J.; Liu, K.-S.; Lai, C.-C.; Liu, Y.-H.; Peng, S.-M.; Cheng, R. P.; Chiu, S.-H. Na+ Ions Induce the Pirouetting Motion and Catalytic Activity of [2]Rotaxanes. *Chem. - Eur. J.* **2017**, *23*, 9756−9760. (c) Zhang, Q.-W.; Zajíček, J.; Smith, B. D. Cyclodextrin Rotaxane with Switchable Pirouetting. *Org. Lett.* **2018**, *20*, 2096−2099. (d) Naranjo, T.; Lemishko, K. M.; de Lorenzo, S.; Somoza, Á.; Ritort, F.; Pérez, E. M.; Ibarra, B. Dynamics of individual molecular shuttles under mechanical force. *Nat. Commun.* **2018**, *9*, 4512. (e) Sluysmans, D.; Lussis, P.; Fustin, C.-A.; Bertocco, A.; Leigh, D. A.; Duwez, A.-S. Real-Time Fluctuations in Single-Molecule Rotaxane Experiments Reveal an Intermediate Weak Binding State during Shuttling. *J. Am. Chem. Soc.* **2021**, *143*, 2348−2352. (f) Kumpulainen, T.; Panman, M. R.; Bakker, B. H.; Hilbers, M.; Woutersen, S.; Brouwer, A. M. Accelerating the Shuttling in Hydrogen-Bonded Rotaxanes: Active Role of the Axle and the End Station. *J. Am. Chem. Soc.* **2019**, *141*, 19118−19129. (g) Stoffel, S.; Zhang, Q.-W.; Li, D.-H.; Smith, B. D.; Peng, J. W. NMR Relaxation Dispersion Reveals Macrocycle Breathing Dynamics in a Cyclodextrin-based Rotaxane. *J. Am. Chem. Soc.* **2020**, *142*, 7413−7424. (h) Corra, S.; de Vet, C.; Baroncini, M.; Credi, A.; Silvi, S. Stereodynamics of E/Z isomerization in rotaxanes through mechanical shuttling and covalent bond rotation. *Chem.* **2021**, *7*, 2137−2150.

(26) (a) Coutrot, F. A Focus on Triazolium as a Multipurpose Molecular Station for pH-Sensitive Interlocked Crown-Ether-Based Molecular Machines. *ChemistryOpen* **2015**, *4*, 556−576. (b) Ragazzon, G.; Baroncini, M.; Silvi, S.; Venturi, M.; Credi, A. Light-powered autonomous and directional molecular motion of a dissipative self-assembling system. *Nat. Nanotechnol.* **2015**, *10*, 70−75. (c) Erbas-Cakmak, S.; Fielden, S. D. P.; Karaca, U.; Leigh, D. A.; McTernan, C. T.; Tetlow, D. J.; Wilson, M. R. Rotary and linear molecular motors driven by pulses of a chemical fuel. *Science* **2017**, *358*, 340. (d) Curcio, M.; Nicoli, F.; Paltrinieri, E.; Fois, E.; Tabacchi, G.; Cavallo, L.; Silvi, S.; Baroncini, M.; Credi, A. Chemically Induced Mismatch of Rings and Stations in [3]Rotaxanes. *J. Am. Chem. Soc.* **2021**, *143*, 8046. (e) David, A. H. G.; Casares, R.; Cuerva, J. M.; Campaña, A. G.; Blanco, V. A [2]Rotaxane-Based Circularly Polarized Luminescence Switch. *J. Am. Chem. Soc.* **2019**, *141*, 18064−18074. (f) Yang, S.; Zhao, C.-X.; Crespi, S.; Li, X.; Zhang, Q.; Zhang, Z.-Y.; Mei, J.; Tian, H.; Qu, D.-H. Reversibly modulating a conformation-adaptive fluorophore in [2]-catenane. *Chem.* **2021**, *7*, 1544−1556.

(27) (a) Abe, Y.; Okamura, H.; Nakazono, K.; Koyama, Y.; Uchida, S.; Takata, T. Thermoresponsive Shuttling of Rotaxane Containing Trichloroacetate Ion. *Org. Lett.* **2012**, *14*, 4122−4125. (b) Berrocal, J. A.; Biagini, C.; Mandolini, L.; Di Stefano, S. Coupling of the Decarboxylation of 2-Cyano-2-phenylpropanoic Acid to Large-Amplitude Motions: A Convenient Fuel for an Acid−Base-Operated Molecular Switch. *Angew. Chem., Int. Ed.* **2016**, *55*, 6997−7001. (c) Ghosh, A.; Paul, I.; Adlung, M.; Wickleder, C.; Schmittel, M. Oscillating Emission of [2]Rotaxane Driven by Chemical Fuel. *Org. Lett.* **2018**, *20*, 1046−1049. (d) Biagini, C.; Fielden, S. D. P.; Leigh, D. A.; Schaufelberger, F.; Di Stefano, S.; Thomas, D. Dissipative Catalysis with a Molecular Machine. *Angew. Chem., Int. Ed.* **2019**, *58*, 9876−9880. (e) Biagini, C.; Di Stefano, S. Abiotic Chemical Fuels for the Operation of Molecular Machines. *Angew. Chem., Int. Ed.* **2020**, *59*, 8344−8354. (f) Ghosh, A.; Paul, I.; Schmittel, M. Multitasking with Chemical Fuel: Dissipative Formation of a Pseudorotaxane Rotor from Five Distinct Components. *J. Am. Chem. Soc.* **2021**, *143*, 5319−5323.

(28) Because we use loosely capped vials as reaction vessels, it is likely that irreversible but slow loss of NH_3 occurs during our rotaxane syntheses, and this may be a crucial factor for the success of the reaction.

(29) (a) Otto, S.; Furlan, R. L. E.; Sanders, J. K. M. Selection and Amplification of Hosts From Dynamic Combinatorial Libraries of Macrocyclic Disulfides. *Science* **2002**, *297*, 590. (b) Black, S. P.; Sanders, J. K. M.; Stefankiewicz, A. R. Disulfide exchange: exposing supramolecular reactivity through dynamic covalent chemistry. *Chem. Soc. Rev.* **2014**, *43*, 1861−1872.

(30) Ashton, P. R.; Bartsch, R. A.; Cantrill, S. J.; Hanes, R. E.; Hickingbottom, S. K.; Lowe, J. N.; Preece, J. A.; Stoddart, J. F.; Talanov, V. S.; Wang, Z.-H. Secondary dibenzylammonium ion binding by [24]crown-8 and [25]crown-8 macrocycles. *Tetrahedron Lett.* **1999**, *40*, 3661−3664.

(31) (a) Hübner, G. M.; Gläser, J.; Seel, C.; Vögtle, F. High-Yielding Rotaxane Synthesis with an Anion Template. *Angew. Chem., Int. Ed.* **1999**, *38*, 383−386. (b) Schalley, C. A.; Silva, G.; Nising, C. F.; Linnartz, P. Analysis and Improvement of an Anion-Templated Rotaxane Synthesis. *Helv. Chim. Acta* **2002**, *85*, 1578−1596.

(32) The unusual kinetic stability of the amidinium rotaxanes also applies to water as a nucleophile; i.e., the rotaxanes are remarkably stable against H_2O. For instance, when we left the reaction mixture of the amidinium rotaxane self-assembly in THF for 3 months at room temperature, the amount of the free thread constantly decreased and we could show that after about 20 days the thread did not convert into the rotaxane anymore, but kept degrading (most likely due to residual water in the solvent) (Figure S39).

(33) (a) Mateo-Alonso, A.; Brough, P.; Prato, M. Stabilization of fulleropyrrolidine N-oxides through intrarotaxane hydrogen bonding. *Chem. Commun.* **2007**, 1412−1414. (b) Gauthier, M.; Coutrot, F. Weinreb Amide as Secondary Station for the Dibenzo-24-crown-8 in a Molecular Shuttle. *Eur. J. Org. Chem.* **2019**, *2019*, 3391−3395. (c) Buston, J. E. H.; Young, J. R.; Anderson, H. L. Rotaxane-encapsulated cyanine dyes: enhanced fluorescence efficiency and photostability. *Chem. Commun.* **2000**, 905−906.

https://doi.org/10.1021/jacs.1c05230
J. Am. Chem. Soc. 2021, 143, 16448−16457